ELSEVIER

Biophysical Chemistry 55 (1995) 197–208

Biophysical Chemistry

Effects of cholesterol on transmembrane water diffusion in human erythrocytes measured using pulsed field gradient NMR

A. Reginald Waldeck [a], M. Hossein Nouri-Sorkhabi [a], David R. Sullivan [b], Philip W. Kuchel [a,*]

[a] *Department of Biochemistry, The University of Sydney, Sydney 2006, N.S.W., Australia*
[b] *Department of Clinical Biochemistry, Royal Prince Alfred Hospital, Camperdown 2050, N.S.W., Australia*

Received 6 July 1994; revised 13 January 1995; accepted 16 January 1995

Abstract

The effect of cholesterol on the diffusional permeability of water in suspensions of human erythrocytes was studied by means of pulsed field gradient NMR, which unlike the relaxation NMR method avoids the use of Mn^{2+} ions. The analysis allows the internal and external diffusion coefficients, as well as the lifetime characterizing the rate of exchange between the two regions, to be extracted from the data. The cholesterol content of the erythrocyte membranes was altered by incubating the cells with sonicated dispersions of cholesterol/dipalmitoyl phosphatidylcholine at 310 K. It was shown that decreasing the molar ratio of cholesterol to phospholipid (C/P ratio) of the membrane, from a mean value of 0.92 for normal cells (controls) to a value of 0.46, had little effect on the intracellular mean residence lifetime and the diffusional permeability. Enriching the cholesterol content of the membrane, however, had a marked effect on the exchange lifetime and the diffusional permeability. At a C/P ratio of ≈ 1.5 the rate of transport was reduced ≈ 3.5-fold. A further increase of the cholesterol content, to a C/P ratio of ≈ 1.9, resulted in an enhancement of the rate of transport back to a normal (control) value, which was characterized by a lifetime of 8–9 ms. The combined inhibition of the water permeability by cholesterol and pCMBS for cells with C/P ratios of 1.44 and 1.54, and by pCMBS alone for cells with a control C/P ratio resulted in the same value for P_d within experimental error.

Keywords: NMR; Water transport; Cholesterol; Diffusion; Mean residence lifetime; Permeability; Hypercholesterolaemia; Liver disease

1. Introduction

The osmotic [1] and diffusional [2] permeabilities of water in erythrocytes of a number of species have been measured using a variety of techniques. The diffusional permeability has been investigated using nuclear magnetic resonance (NMR) relaxation time measurements [3–5], total NMR lineshape analysis [6], and pulsed field gradient (PFG) NMR [7,8]. Water transport in human erythrocytes is extremely rapid, and this is believed to be important in preventing osmotic rupture when the cells pass into and then out of the vessels of the renal medulla where the osmotic pressure of the surroundings is ≈ 4 times

* Corresponding author. Tel. (+61-2)3513709, fax. (+61-2)3514726.

SSDI 0301-4622(95)00007-0

the normal plasma value [9]. Water transport in human erythrocytes is characterized by channel-mediated transport, on the basis of its high osmotic permeability ($P_f \approx 0.02$ cm s^{-1}), high ratio of osmotic-to-diffusional permeability ($P_f/P_d \geq 3$), a low activation energy ($E_a = 18.8$ kJ mol^{-1}), and strong inhibition of P_f ($\approx 90\%$) by mercurial sulfhydryl reagents [10]. Recently, a 28 kDa channel-like intrinsic protein (CHIP 28) from human erythrocytes was isolated and cloned; it is now thought to embody nearly 100% of the permeability to water in these cells [1,10–14].

The effects of cholesterol and other sterols on the rate of permeation by water and solutes of cellular, vesicular, and synthetic membranes, whether by passive, facilitated, or active mechanisms, have been studied extensively [15–24]. The 'condensing' and 'ordering' effects of cholesterol on lipids in the membrane at temperatures above the phase transition temperature (T_m) of the membrane are generally believed to be responsible for a decrease in the permeability of solutes that diffuse through the lipid part of the membrane (for reviews see [25,26]). However, in some cases of protein-mediated transport of solutes, specific *sterol*–protein interactions must be considered in order to account for the modulation of the rates [17,23,24,27]. 'Interstitial water pores' which presumably are caused by transient bilayer defects have been postulated to account for the anomalously high permeability to water of synthetic membranes [28,29], but they are also likely to play a significant role in biological membranes [30,31]. The osmotic permeability of water transport across the membranes of human erythrocytes is not affected by (extensive) depletion of membrane cholesterol [16], but increasing the cholesterol content of the membrane by ≈ 30–60% decreases the permeability considerably [22].

In this study, we applied PFG NMR to measure the diffusional exchange of water across the membranes of human erythrocytes that had been depleted or enriched with cholesterol. The PFG NMR technique has the virtue that it is chemically 'non-invasive', in contrast to the 'manganese doping' NMR technique [4,5]. Our results are in qualitative agreement with those previously reported on the effects of cholesterol on the rate of water transport in erythrocytes [16,22], but the permeability was shown here not to be a monotonically decreasing function of the molar ratio of cholesterol to phospholipid (C/P ratio). Furthermore, the 3–4-fold reduction in the water permeability observed with erythrocyte membranes with C/P ratios of ≈ 1.5, is likely to be clinically significant for patients with liver disease [32] and hypercholesterolaemia [33].

2. Theory

The expression relating the attenuation of the NMR signal (R) of the species under study to the experimental parameters in a two-compartment system, ignoring relaxation-time differences between the two regions, and allowing for molecular exchange between the two regions, is described by a sum of two exponentials [34–37]:

$$R = R_1 + R_2 = P_1 \exp(-KD_1\Delta) + P_2 \exp(-KD_2\Delta) \quad (1)$$

where D_1, D_2, P_1, and P_2 are the 'apparent' self-diffusion coefficients and population fractions (relative signal intensities), which are related to the *real* system parameters, by:

$$D_1 = \tfrac{1}{2}\Big\{D_e + D_i + 1/K(1/\tau_e + 1/\tau_i) - \sqrt{([D_i - D_e + 1/K(1/\tau_i - 1/\tau_e)]^2 + 4/K^2\tau_e\tau_i)}\Big\}$$

$$D_2 = \tfrac{1}{2}\Big\{D_e + D_i + 1/K(1/\tau_e + 1/\tau_i) + \sqrt{([D_i - D_e + 1/K(1/\tau_i - 1/\tau_e)]^2 + 4/K^2\tau_e\tau_i)}\Big\}$$

$$P_1 = 1 - P_2$$

$$P_2 = (P_e D_e + P_i D_i - D_1)/(D_2 - D_1)$$

$$K = \gamma^2 g^2 \delta^2$$

where D_e and D_i are the diffusion coefficients of the molecules in the extra- and intracellular compartments, respectively; δ denotes the duration of the magnetic field gradient pulse, Δ the time interval between the leading edges of the field gradient pulses, g the magnitude of the field gradients, and γ the magnetogyric ratio of the observed nuclide. P_e and P_i are the relative extracellular and intracellular population fractions, respectively, which, for erythrocytes are given by:

$$P_e = (1 - Ht)/[Ht(\alpha - 1) + 1] \quad (2a)$$

$$P_i = \alpha Ht/[Ht(\alpha - 1) + 1] \quad (2b)$$

where α denotes the fraction of the cell volume available to water and solutes, and has the value 0.717 for water [38], and Ht denotes the haematocrit of the suspension. τ_e and τ_i are the mean residence lifetimes in the corresponding compartments; τ_e can be cancelled from Eq. 1 by noting that $\tau_e = P_e\tau_i/P_i$. Eq. 1 is based on the assumptions that: (1) the intercompartment exchange rate constants are much greater than the transverse relaxation rate constants of the nuclide under study; i.e., $k_j \gg (T_{2,j})^{-1}$ (j = i, e); and (2) the magnetization-phase dispersion (due to diffusion) during δ is negligible compared with that occurring during Δ; i.e., $\Delta \gg \delta$.

The above expressions will simplify in the limits of slow exchange (lim $\tau_j \to \infty$) to give $D_1 = D_e$, $D_2 = D_i$, $P_1 = P_e$, and $P_2 = P_i$, and in the very rapid exchange limit (lim $\tau_j \to 0$) $D = P_e D_e + P_i D_i$, thus resulting in a single exponential for Eq. 1. In both these latter cases, τ_j cannot be determined from these equations (see Fig. 6).

Eq. 1 is simplified significantly in the case of small regions of high mobility. With respect to erythrocytes, a suspension with a relatively high Ht, such that the mean square displacement of the species diffusing within the extracellular medium is (still) much greater than that in the cytoplasm; i.e., $P_i \gg P_e$ and $D_e \gg D_i$ leads to the simplification. Thus, Eq. 1 simplifies to a single-exponential function that is characterized by an 'effective' diffusion coefficient that is given by [39,40]:

$$D_{\text{eff}} = D_i + \frac{P_e D_e}{KP_e D_e \tau_i + 1} \tag{3}$$

and hence, the normalized signal-attenuation is given by:

$$R = \exp\left\{ -K \left(D_i + \frac{P_e D_e}{KP_e D_e \tau_i + 1} \right) \Delta \right\} \tag{4}$$

From Eq. 3 it is clear that for the limiting cases of very small or very large values of K ($\propto$ gradient intensity), which correspond to the inequalities $K \ll (P_e D_e \tau_i)^{-1}$ and $K \gg (P_e D_e \tau_i)^{-1}$, D_{eff} is given by $(D_i + P_e D_e)$ and D_i, respectively. In addition, Eq. 4 allows the estimation of τ_i by graphical analysis of the double exponential function that characterizes the PFG NMR data that are recorded from solutes that diffuse in two-region systems (see Fig. 2 and Results for details).

Finally, the diffusional efflux permeability (P_d) is calculated from τ_i as follows:

$$P_d = (\tau_i)^{-1}\left(V^{\text{cell}}/A^{\text{cell}}\right) = k_e\left(\alpha \text{MCV}/A^{\text{cell}}\right) \tag{5}$$

where V^{cell}, A^{cell}, k_e and MCV denote the volume of a single erythrocyte that is accessible to solutes and water, the membrane surface area of a single cell, the (pseudo) first-order exchange rate constant, and the mean cell volume, respectively. Eq. 5 applies to the case in which the transport is not 'diffusion-limited' (i.e., 'barrier-limited' exchange). This condition is fulfilled, for example, if the cells are approximated by spheres of a comparable volume and the inequality $3D\tau_i/R^2 > 1$ holds, where D is the unrestricted (intrinsic) diffusion coefficient [41]. In the case of water diffusion in a human erythrocyte $3D\tau_i/R^2 = 3.36$, using $R = 3$ μm [8], $D = 1.12 \times 10^{-9}$ m^2 s^{-1} (value obtained from a cell lysate with $Ht = 0.97$ prior to lysing the cells), and $\tau_i = 9$ ms. Thus, the membrane permeability is rate-limiting for the transmembrane exchange of water in human erythrocytes; in this situation τ_i is referred to as the exchange lifetime.

3. Materials and methods

Modification of the cholesterol (Sigma Chem. Co., St Louis, MO, USA) content of the erythrocyte membranes was achieved by using an adaptation [42] of the procedure of Grunze and Deuticke [19] and Cooper et al. [43]. Briefly, the method involved incubating (7–45 h; 310 K) erythrocytes ($Ht = 0.10$; from freshly drawn venous blood from one healthy donor) in a suspension of small unilamellar vesicles (SUV) consisting of dipalmitoyl phosphatidylcholine (DPPC; Sigma) or DPPC and cholesterol [1:1–1.5 (w/w)] for depletion or enrichment, respectively. The incubation buffer contained 100 mM KCl, 50 mM NaCl, 40 mM sucrose, 2.5 mM NaH_2PO_4, 10 mM Na_2HPO_4, 10 mM glucose, and 5 mM inosine, pH 7.4.

NMR samples were prepared, after the incubations, by centrifugal washing of the erythrocytes three times ($3000 \times g$; 10 min; 273 K) in phosphate

buffered saline (PBS) supplemented with 10 mM glucose, pH 7.4, which was presaturated with CO by bubbling it with the gas for 10 min. The *Ht* was adjusted, if necessary, to 0.75–0.85. These samples were then placed in microcylindrical 'diffusion cells' (volume ≈ 490 μl; Wilmad Glass Co., Buena, NJ, USA) and kept at 273 K before incubating them (10 min; 310 K) prior to NMR measurement. When the water transport was inhibited, the samples had been incubated with ≈ 1 mM (with respect to the total sample volume) of the sulfhydryl reagent parachloromercuribenzenesulfonate (pCMBS; Sigma) for 45 min at an *Ht* of ≈ 0.10. They were then washed an additional three times in PBS prior to adjustment of the final *Ht*. Solutions of pCMBS were prepared freshly, and care was taken to minimize exposure of the compound to light. Following NMR measurements, the number of cells in the suspensions were determined in triplicate, at least, using a Sysmex Microcell Counter CC-130 (Toa Medical Electronics, Kobe, Japan).

NMR spectra were recorded on a Bruker AMX 400 wide-bore NMR spectrometer equipped with a multinuclear diffusion probe. The PFG apparatus that was used for the generation of the magnetic field gradient pulses was also supplied by Bruker, and performed as described previously [44]. A modified [45] pulsed field gradient longitudinal eddy current delay (PFGLED) pulse sequence [46] was used to record the PFGNMR spectra. The values of the PFGNMR parameters in the 'little delta' experiments were: $\delta = 0.003$–3 ms with increments of 0.25 ms; $\Delta = 100$ ms; $g = 636$ mT m^{-1}; $2\tau = 40$ ms; $T = 80$ ms; $T_e = 20$ ms; and $\delta_e = 17$ ms. The values of the PFG parameters in the 'variable g' experiments were identical to those in the 'little delta' experiments, except that $\delta = 3$ ms and $g = 0.2$–636 mT m^{-1}. The temperature of the samples was kept constant to ± 1 K by thermally regulated nitrogen gas. NMR spectra were acquired with a spectral width of 4 kHz with 2 K datapoints, an intertransient delay of 2.0–2.5 s, a $\pi/2$-pulse duration of ≈ 24 μs, and

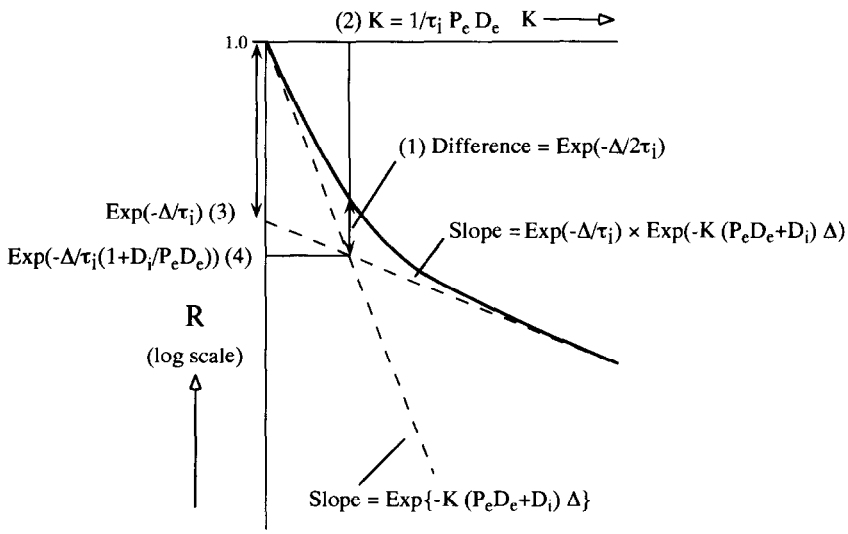

Fig. 1. Stylised graph of the echo-attenuation of an NMR signal from a solute diffusing in a system consisting of two regions versus the 'aggregated' parameter K ($= \gamma^2 g^2 \delta^2$), where one region (e) is of larger volume and is characterized by a high diffusivity, and the other region (i) is characterized by a low diffusivity; viz., $P_i \gg P_e$ and $D_e \gg D_i$. The solid line in the graph is the sum of two exponentials and the asymptotes that characterize the limiting exponential functions, at high and low values of K, respectively, are denoted by the dotted lines. The curve is also characterized by four other relationships, from which D_e, D_i, and τ_i may be estimated (when P_e is known) as follows: 1, From the point of intersection of the second (less steep) asymptote and the R-ordinate [relationship (3)]; this value is equal to $\exp(-\Delta/\tau_i)$ and it represents the fraction of the nuclear population which has *not* left the internal region during the time-interval Δ. 2, The point of intersection of the two asymptotes is characterized by $K = (\tau_i P_e D_e)^{-1}$ [relationship (2)]. 3, The value of R at $K = (\tau_i P_e D_e)^{-1}$ is given by $\exp(-\Delta/\tau_i(1 + D_i/P_e D_e))$ [relationship (4)]. And 4, The difference between $\ln R$ and the second asymptote ($\ln R_2$) is characterized by a decrease from a value of (Δ/τ_i) for $K = 0$ to $(\Delta/2\tau_i)$ for $K = (\tau_i P_e D_e)^{-1}$ [relationship (1)].

averaged over 8–32 transients. A line-broadening factor of 5 Hz was applied to the data, prior to Fourier transformation, to increase the apparent signal-to-noise ratio of the spectra. An automatic baseline correction (third-order polynomial function) was used after phase-correction of the spectra.

The C/P ratio of the erythrocyte membranes was determined by extraction of the membrane lipids and measuring the concentrations of cholesterol by HPLC and that of total phospholipid by previously described procedures [42].

The value of A^{cell} for a normal human erythrocyte that was required for the calculation of P_d, was taken to be 1.43×10^{-6} cm^2 [47]; this value was 'adjusted' for the cholesterol-depleted and cholesterol-enriched erythrocytes by using a 0.22% decrease/increase in surface area for a 1% decrease/increase in cholesterol content of the membrane [20,48]. The (minor) changes in the cell volume were corrected for by adjustment of α in Eqs. 3a and 3b, as described previously [49].

Weighted $(1/R^2)$ non-linear least-squares regression analysis of Eq. 1 (lim $\tau_j \rightarrow \infty$) onto the PFG data was performed on a Macintosh Quadra computer using the program Regression (Marquardt algorithm). The estimate of errors in the parameter values that were determined from the analysis, were based on estimates of the errors in the experimental variables using the process of 'propagation of errors', as described previously [50]. The values of parameters and their associated errors are quoted as the mean ± SD (standard deviation). Theoretical plots of Eq. 1, showing the relationship between the signal-attenuation (R) and τ_i as a function of the parameter $(\delta \times g)^2$ (Fig. 6), were generated using the computer package Mathematica [51].

4. Results

Fig. 1 shows a schematic representation of the attenuation of an NMR echo-signal that is detected from a solute or solvent in a composite system consisting of an internal and an external region (compartment), in which the fraction of the nuclear population in the internal region is much greater than that within the external one. Also, the molecular motion of the solute or solvent within the internal

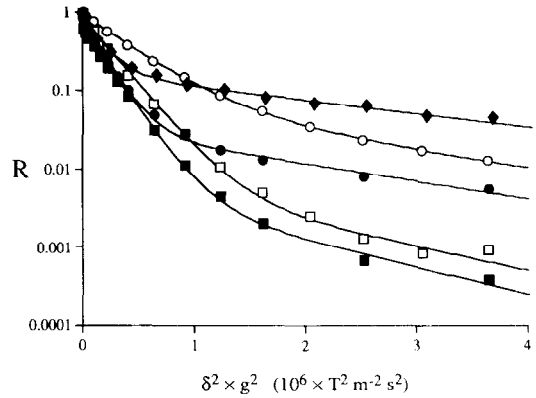

Fig. 2. PFG NMR signal intensities that were recorded from water diffusing in human erythrocytes at 310 K versus the square of the product of the duration, δ, and the magnitude, g, of the field gradient pulses, $(\delta \times g)^2$. The lines were obtained by weighted $(1/R^2)$ non-linear least-squares regression of Eq. 1 (lim $\tau_j \rightarrow \infty$). Data from cells ($Ht = 0.78$) which had been incubated with ≈ 1 mM pCMBS (control, C/P = 0.84) are denoted by ○. ◆ denote data from cells characterized by a C/P ratio of 1.44. ● denote data from erythrocytes ($Ht = 0.76$) of which the membranes were depleted of cholesterol (C/P = 0.46). □ denote data from erythrocytes ($Ht = 0.76$) of which the membranes had been enriched with cholesterol (C/P = 1.88). ■ denote data from control cells ($Ht = 0.75$; C/P = 0.80).

region, is characterized by a much lower value of the diffusion coefficient than that in the external region; thus, $P_i \gg P_e$ and $D_e \gg D_i$. The curve in Fig. 2 is characterized by four relationships from which τ_i may be estimated. D_e and D_i can be estimated from the slopes of the curve (values plotted in Fig. 5) at very low and very high values of the parameter K; i.e., in domains of K where the rapidly and slowly decaying exponentials dominate the value of the function (see Theory). The exchange lifetimes, and their respective standard deviations, were estimated using all four relationships. The lowest mean coefficient of variation of all four estimates, viz. 21.7%, was obtained using relationship (1), the other mean relative errors were 24.5%, 22.0%, and 32.0% for relationships (2), (3), and (4), respectively. The weighted mean value of τ_i ($n = 3$), obtained using the weighting factor 1/variance, that was estimated for the control cells (not incubated), was 8.8 ± 2.0 ms. Thus, using relationship (1), the estimate of τ_i was the most precise and was also that which was most in agreement with previous estimates. Previous estimates of τ_i in suspensions of erythrocytes at 310

K, which had been corrected for artefacts related to the experimental and mathematical procedures that were used in various individual studies, range between 6.0 and 9.6 ms [5]. The values that were calculated from the other relationships were all higher.

Fig. 2 shows PFG data that were recorded from control cells in the absence and presence of the water transport inhibitor pCMBS, of erythrocytes of which the membranes were either extensively depleted or enriched with cholesterol (C/P ratio = 0.46 and 1.88, respectively), and of cholesterol-enriched cells with a C/P ratio of 1.44. Note the substantially smaller signal-attenuation in the presence of pCMBS, and at a C/P ratio of 1.44 compared with that of the controls. This was caused by inhibition of the transport (increase in τ_j). Note that the data from cells with a C/P ratio of 0.46 also appear to be characterized by a reduced τ_i-value relative to those of the control cells (see also Fig. 4). The parameter estimates (P_1, P_2, D_1, and D_2) that were obtained from the regression analysis (Eq. 1; lim $\tau_j \rightarrow \infty$) were used for further analysis with Eq. 5 in terms of the relationships that are given in Fig. 1.

Fig. 3 shows the dependence of the exchange lifetime (τ_i) versus the C/P ratio in human erythrocytes, at 310 K. Depletion of membrane cholesterol appeared not to have any effect on the rate of diffusional exchange (proportional to τ_i^{-1}) at C/P ratios ranging from 0.5 to 1.1; the C/P ratio of control cells was 0.92 ± 0.14 ($n = 4$). Enrichment of the cholesterol content of the membrane to a C/P ratio of 1.44, however, resulted in approximately a 3.5-fold increase of the exchange lifetime, to a value of 28 ms. A further increase in the C/P ratio reversed this trend, such that at a C/P ratio of ≈ 1.9,

Table 1
Efflux permeability coefficients [a] characterizing diffusional water transport in human erythrocytes as a function of the C/P ratio of their membranes

(C/P) [b]	% change in (C/P) [c]	k_c (s^{-1})	P_d	P_d + pCMBS [d]
0.46	−43	74 ± 10	4.4 ± 0.6	
0.48	−40	108 ± 11	5.8 ± 0.6	
0.53	−34	113 ± 27	5.7 ± 1.4	
0.56	−40	78 ± 7	4.4 ± 0.4	
0.61	−24	121 ± 20	6.0 ± 1.0	
0.63	−32	110 ± 34	5.5 ± 1.7	
0.69	−26	106 ± 20	5.5 ± 1.0	
0.80 [e]	0	120 ± 30	5.7 ± 1.4	
0.84 [e]	0	n.d.	n.d.	0.75 ± 0.15
0.85	−9	114 ± 27	5.9 ± 1.4	
0.93 [e]	0	103 ± 24	5.3 ± 1.2	
1.11 [e]	0	118 ± 25	5.1 ± 1.4	
1.11	0	114 ± 32	5.0 ± 1.0	
1.21	+9	102 ± 29	5.2 ± 1.5	
1.27	+51	52 ± 12	2.1 ± 0.5	
1.35	+22	82 ± 13	4.6 ± 0.7	
1.44	+71	35 ± 8	1.4 ± 0.3	0.74 ± 0.11
1.54	+83	56 ± 11	2.1 ± 0.4	0.76 ± 0.18
1.76	+110	79 ± 16	2.7 ± 0.5	
1.88	+69	115 ± 45	6.2 ± 2.5	

[a] Diffusional efflux permeability coefficients ($10^3 \times$ cm s^{-1}) ± SD. The total number of samples was 20. Blood was taken from a single donor on four different days (i.e., two depletion and two enrichment experiments including controls); one NMR experiment was performed on each of the samples.

[b] Molar ratio of cholesterol to phospholipid (C/P ratio).

[c] Percentage change in the molar ratio of cholesterol to phospholipid with respect to the corresponding control sample.

[d] Efflux permeability coefficients in the presence of pCMBS (≈ 1 mM with respect to the total volume of the sample).

[e] Control sample.

n.d. not determined.

the value of τ_i was the same as that for the control cells.

Table 1 lists the diffusional efflux permeabilities (P_d) that were calculated using Eq. 5, together with their corresponding C/P ratio, which is also quoted relative to that of control cells. The latter is given merely as an indication of the range over which the C/P ratio may vary given the (intra-individual) variation that exists; of course, its absolute value is the parameter which is most directly related to P_d. A graph of $(P_d)^{-1}$ versus the C/P ratio of the erythrocyte membranes (not shown) showed the same form as the dotted line in Fig. 4. The value of P_d in control cells was $5.4 \pm 0.4 \times 10^{-3}$ cm s^{-1} ($n = 3$), and this value is in reasonable agreement with previous estimates of this parameter ([2,4] and references therein). The values of P_d that were measured in the presence of pCMBS (one control and two cholesterol-enriched samples) were not significantly different from each other, and corresponded to $\tau_i \approx 67$ ms. Thus, the reduction in the water permeability due to the higher cholesterol concentration of the erythrocyte membrane did not add linearly to the inhibition that was caused by pCMBS.

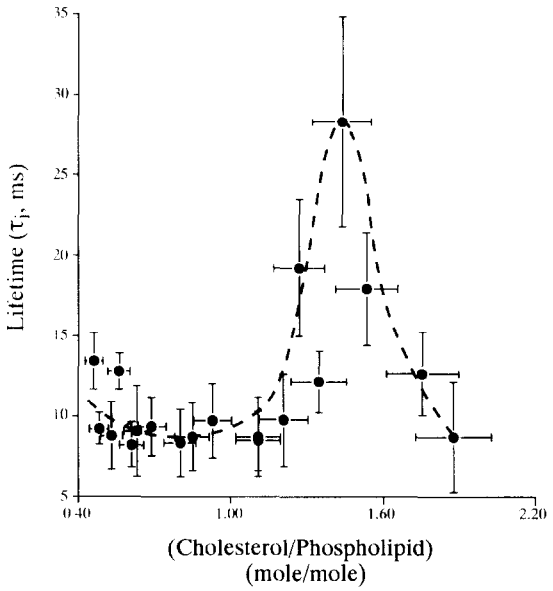

Fig. 3. Graph of the cytoplasmic mean residence lifetime (τ_i) that was calculated using relationship (1) (see Fig. 1) versus the molar ratio of cholesterol to phospholipid, at 310 K. The abscissa error bars indicate a coefficient of variation of 8% in the C/P ratio and the ordinate error bars indicate the relative error that was estimated from the analysis of Eq. 4, as described in Results. The dotted line was drawn empirically, and it serves to guide the eye.

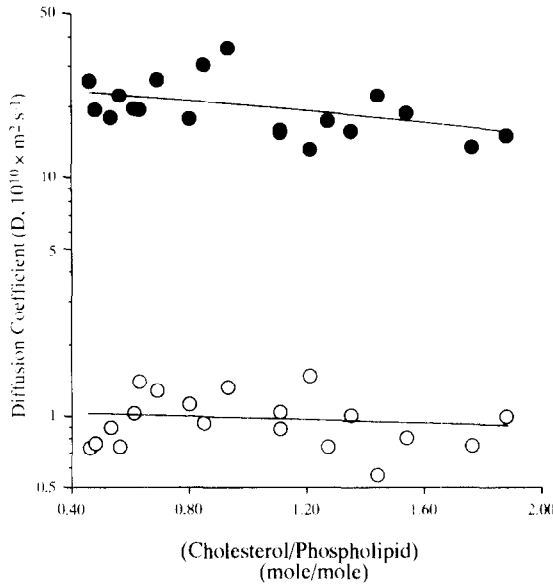

Fig. 4. Graph of the estimates of intra- and extracellular diffusion coefficients (D) of water versus the molar ratio of cholesterol to phospholipid, measured at 310 K. ● and ○ denote the values of the extracellular and the intracellular diffusion coefficients, respectively. The mean coefficients of variation of the extra- and intracellular diffusion coefficients were 5% and 12%, respectively. The trend of the data is illustrated by the lines of 'best fit' that were obtained by linear regression analysis. The individual ordinate error bars were omitted because most fell within the circumference of the datapoints.

Fig. 4 shows a graph of the values of the intra- and extra-erythrocyte diffusion coefficients (D) of water versus the C/P ratio of the erythrocyte membranes. The values of the diffusion coefficients of water inside, and outside the cells, varied by approximately an order of magnitude; specifically, D_i and D_e of the control samples were $1.1 \pm 0.1 \times 10^{-10}$ m^2 s^{-1} and $2 \pm 1 \times 10^{-9}$ m^2 s^{-1} ($n = 3$), respectively. The mean Ht of the control samples was 0.77 ± 0.10, the MCV was 90.6 ± 6.0 fl ($n = 4$), the mean Ht of the samples which were incubated with pCMBS was 0.76 ± 0.06, their corresponding MCV amounted to 97.6 ± 5.5 fl ($n = 3$), while the mean Ht of all the samples was 0.77 ± 0.07, with a corresponding mean MCV of 91.8 ± 5.4 fl ($n = 20$).

Fig. 5 shows the theoretical 'behaviour' of Eq. 1 with respect to the mean residence lifetime inside the

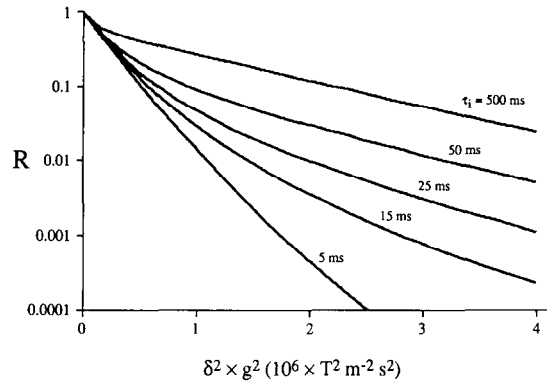

Fig. 5. Theoretical plots of Eq. 1 showing the relationship between the signal-attenuation (R) and the internal mean residence lifetime (τ_i) as a function of the square of the product of the duration, δ, and the magnetic field strength, g, of the gradient pulses $(\delta \times g)^2$. The values of the parameters that were used in the simulation were: $P_e = 0.294$; $P_i = 0.706$ [values corresponding to the mean *Ht* of the control samples (0.77)]; $D_e = 2.0 \times 10^{-9}$ m^2 s^{-1} (limiting value of the obstructed diffusion coefficient according to the model of Lindman and Nilsson [57] and Jönsson et al. [58]; $D_i = 1.1 \times 10^{-10}$ m^2 s^{-1} (mean value of the control samples); and $\Delta = 0.1$ s. Note the 'sensitivity' of D_1 [slope of the curve at large values of $(\delta \times g)^2$] on values of $\tau_i \leq 15$ ms.

cell. The plots show that D_1 (the slope of the slowly decaying exponential) varies markedly across a broad range of exchange lifetimes, and is more 'sensitive' to changes in this parameter than D_2. Importantly, the determination of τ_i is prone to error in data for which the exchange rates are rapid, as is the case for water transport in cells, (i.e., lim $\tau_j \rightarrow 0$); a small uncertainty in D_1 results in a large error in the estimate of τ_i. Thus, the accuracy of the estimate of τ_i becomes 'problematic' for $\tau_i < 15$ ms with the PFG NMR parameters that we were constrained to use on technical grounds.

5. Discussion

5.1. The effects of cholesterol on the water permeability of membranes

The interactions of cholesterol with other constituents of (bio)membranes are manifold and complex (for reviews see [25,26,52]). The *molecular* nature and effects of interactions of sterols with different membrane-spanning proteins remain largely obscure. However, the opposite effects of cholesterol on various facilitated transfer processes in the erythrocyte membrane [21] are indicative of different 'types' of cholesterol–protein and/or cholesterol-induced lipid-mediated interactions.

There are relatively few studies which have been concerned with the effects of cholesterol on the permeability of *water* across membranes. The pioneering work of Finkelstein and Cass [15] demonstrated that cholesterol markedly reduces P_f of thin lipid membranes up to a C/P ratio of $\approx$ 4:1. To our knowledge, no one had previously investigated the effects of cholesterol on the *diffusional* water permeability of *biological* membranes. The reports on the osmotic permeability of water through membranes of human erythrocytes [16,22] are consistent with our finding, that, for C/P ratios between 0.5 and 1.2, cholesterol does not alter the permeability of the membrane to water. In contrast, (further) moderate enrichment of the membrane with cholesterol leads to a significant reduction in water permeability ([22]; this report). At higher C/P ratios, one or more effects which oppose the trend that is evidenced at C/P ratios between 1.25 and 1.50, must exist. These effects caused P_d to increase again back to a normal value at C/P ratios of $\approx$ 1.8–2.0. It is conceivable that the same type of transient defects that have been postulated to occur in proteoliposomes, at protein–lipid interfaces [30,31], dominate the effects exhibited by cholesterol for C/P ratios $\leq$ 1.5, in erythrocytes with C/P ratios > 1.5. Hence, at C/P ratios > 1.5 the increased water permeability, relative to that for C/P ratios $\leq$ 1.5, could be due, in part, to interstitial water pores. The fact that there appears to be a fraction of erythrocyte cholesterol which can be removed or incorporated ($\approx$ 30–50%; C/P $\approx$ 0.5–1.2), which does not have any appreciable effect on the osmotic [16] or diffusional [this report] water permeability, seems to suggest that there are two (or possibly even more) pools of membrane cholesterol in erythrocytes. This possibility has previously been suggested in relation to solutes permeating the mammalian erythrocyte membrane via simple diffusion [19]. Of particular interest, is the study by Kutchai and coworkers [22], because they found that the 'hydraulic conductivity', L_p, which is equal to $P_f V_w / RT$, where V_w is the partial molar volume of water, decreased by 37% when the C/P ratio was

increased by 31 (mol) %, but was lowered only by 26% when the C/P ratio was increased by 65%. These authors discarded the possibility of a particular trend in the data, probably because only two datapoints (C/P ratios) were obtained. They also established that 'spur' cells with a C/P ratio which was twice that of non-pathological cells, (the actual C/P ratio was not mentioned), were characterized by a normal value of L_p. Although these results are circumstantial to a certain extent, in that only three C/P ratios were studied, they are in qualitative agreement with the measurements of P_d described here (see Table 1). No major changes in the measured mean cell volumes of the cells with changes in membrane cholesterol content were observed. However, parallel changes in the surface area of the erythrocytes were predicted according to previously established procedures [20,48]. These variations in erythrocyte surface area have been determined from calculations that are based on changes in the osmotic fragility of the cells [20], as well as from critical-hemolytic-volume measurements [48], and they are consistent with the fact that the cholesterol content of a normal erythrocyte occupies 20–25% of the total membrane surface area. A possible source of error that is introduced into the values of P_d by using this procedure may result from a difference in the phospholipid content of the different samples, but it is thought to be negligible compared with the coefficients of variation of the estimates of the exchange lifetimes.

There is theoretical ([25] and references therein), as well as some experimental evidence for the heterogeneous distribution of cholesterol in the membranes of erythrocytes ([52] and references therein). Thus, the 'expendable' pool of cholesterol may be the one that is associated with the 'bulk' lipid, and it affects the fluidity of the membrane but it does not have a significant effect on the CHIP 28-mediated permeability of the membrane to water. Recently, Zeidel et al. [53] have shown that cholesterol has no effect on CHIP 28-mediated osmotic water flow in proteoliposomes at 5 (mol) %, and 15 (mol) % cholesterol. The higher sterol concentration amounts to a C/P ratio of ≈ 0.2; a ratio which cannot be obtained in erythrocytes. However, their results for the reconstituted water channel is consistent with the general conclusion that the water permeability of cholesterol-depleted erythrocytes appears not to be different from those of cells with a normal C/P ratio ([16]; this report). In the case of extensive enrichment, and perhaps, in red blood cells as opposed to proteoliposomes, also in the case of extensive depletion, a second pool of cholesterol might be affected, which preferentially self-associates, associates with proteins, and/or with sphingomyelin [27]. However, the association of cholesterol with proteins does not necessarily have to be with CHIP 28 alone, as the putative interstitial water channels at the protein–lipid interfaces probably represent a general transient protein–lipid packing defect [30]. This second, non-expendable pool of membrane cholesterol, would then be the principal modulator of the permeability of the erythrocyte membrane to water, in that extensively enriching it may lead to an increase in transient packing defects, while thorough depletion might cause this pool (domain) to become slightly more impermeable.

The combined inhibition of the water permeability by cholesterol and pCMBS for cells with C/P ratios of 1.44 and 1.54, and by pCMBS alone for cells with a control C/P ratio resulted in identical values for P_d within experimental error (see Table 1). Exogenous cholesterol enhances the availability of sulfhydryl groups in intrinsic membrane proteins, and this increase in their exposure to the bordering aqueous medium may result in increased protein–water interactions [55]. If it is assumed that this increase in protein–water interactions has a positive effect on P_d, then a saturating concentration of pCMBS would decrease the number of 'extra' exposed sulfhydryl groups. This would bring about a net reduction of P_d of the cholesterol-enriched samples, to a value that is similar to that of the control sample.

5.2. *PFG NMR as an analytical tool for measuring the P_d of water transport in erythrocytes*

The present work appears to be the first in which Eq. 4 has been applied to study molecular exchange taking place in a *biological* system. The assumption underlying Eq. 1, that the values of the exchange rate constants need to be much greater than the relaxation rate constants, was satisfied, because the T_2 of water inside erythrocytes is ≈ 160 ms [5], and this value sets a lower limit for the value of the corresponding

T_1; the extracellular nuclear relaxation times are longer (≥ 0.5 s; [5]), because, amongst other phenomena, of the fewer less mobile sites to which water may bind outside the cells. The assumption that the magnetization-phase dispersion during δ is negligible, was satisfied because $\delta \leq 3\%$ of the value of Δ. A similar situation occurred in the experiments that are described here, in that, $P_i/P_e \approx 2.9$ and $D_e/D_i \approx 18$. Perhaps, the requirement that the fraction of the whole nuclear population that is intracellular needs to be much greater than the extracellular one, was not perfectly met, but performing the experiments at very high Ht was thought to jeopardize the assumption that $D_e \gg D_i$. The unbounded self-diffusion coefficient (D_0) of water at 310 K is 3.05×10^{-9} m^2 s^{-1} [56]. The extracellular diffusion coefficient can be estimated by applying an obstruction correction factor that takes into account the excluded volume fraction that is occupied by the obstructing particles (i.e., erythrocytes). When the shape of a human erythrocyte is approximated by an oblate ellipsoid, with an axial ratio of $\approx$ 1:4, it can be inferred that with an obstructing volume fraction of 0.77 (the average Ht of all the samples) the 'effective' extracellular diffusion coefficient is close to the limiting (asymptotic) value of $0.67 \times D_0$ [57,58], which is equal to 2.04×10^{-9} m^2 s^{-1}. This value is in good agreement with the average value that was estimated for the control samples (2×10^{-9} m^2 s^{-1}; see also Fig. 5), and thus, the perceived reliability of the values of D_e that were estimated using Eq. 4 was enhanced. A value of $7.34 \pm 0.63 \times 10^{-11}$ m^2 s^{-1} was obtained for D_i in the presence of pCMBS (using Eq. 1; lim $\tau_j \to \infty$); this value provides a rough (over) estimate of the actual D_i that would be measured with $\Delta = 100$ ms in the case of purely reflecting boundaries (i.e., lim $\tau_i \to \infty$). This estimate of D_i (for $\Delta = 100$) is in reasonable agreement with the values that were obtained by analysis of the data using Eq. 4, as shown in Fig. 5, and together with the theoretical estimate of D_e it indicates that the assumption that $D_i \ll D_e$ was met.

As shown in Fig. 1, there are, in principle, four relationships between τ_i and R or τ_i and K, from which τ_i may be calculated. The mean coefficients of variation of the τ_i-data were calculated from each of the four relationships by propagation of the error estimates in the parameters P_1, P_2, D_1, and D_2 that were obtained from the weighted non-linear least-squares regression of Eq. 1 (lim $\tau_j \to \infty$) onto the data. This analysis demonstrated that the most accurate estimates of τ_i were obtained using relationship (1) (see Fig. 2). This result was expected, because this relationship incorporates the value of (R; i.e., $R_1 + R_2$) at $K = (\tau_i P_e D_e)^{-1}$, which is recorded with greater accuracy (signal-to-noise ratio) than the value of R_2 at the same value of K, which is the only value that is used in the calculation of τ_i by means of the other three relationships. More specifically, relationship (1) yields an estimate of τ_i from the difference in the values of $\ln(R_1 + R_2)$ at $K = (\tau_i P_e D_e)^{-1}$ and $\ln R_2$, which means that its estimate is essentially made from that of R_1 at $K = (\tau_i P_e D_e)^{-1}$. Because the value of R_1 at $K = (\tau_i P_e D_e)^{-1}$ is (much) greater than the value of R_2 at $K = (\tau_i P_e D_e)^{-1}$, it is therefore less prone to error.

Finally, the results showed that Eq. 4 describes reasonably well the experimental situation that is encountered in suspensions of erythrocytes of $Ht \approx$ 0.75–0.85, and that the relationship (1); [$\ln R - \ln R_2 = (\Delta/2\tau_i)$] which holds at $K = (\tau_i P_e D_e)^{-1}$ yields the most precise (and accurate) estimate of τ_i.

5.3. Conclusions

Our results showed that in human erythrocytes: (1) the intracellular mean residence lifetime that characterizes the rate of water transport under equilibrium exchange conditions is a non-monotonic function of the molar ratio of cholesterol to phospholipid of the membranes. More specifically, at low C/P ratios τ_i^{-1} and P_d were not affected, while at a C/P ratio of $\approx$ 1.5, τ_i^{-1} and P_d were reduced $\approx$ 3.5-fold; a further increase in the C/P ratio resulted in an increase of both τ_i^{-1} and P_d, and a normal (control) value was reached at a C/P ratio of $\approx$ 1.9. (2) The combined inhibition of the water permeability by cholesterol and pCMBS for cells with C/P ratios of 1.44 and 1.54, and by pCMBS alone for cells with a control C/P ratio resulted in similar values for P_d. (3) The PFG NMR method of measuring τ_i using Eq. 4, provided a simple, rapid, reliable, and non-invasive method for determining the rate of water transport and diffusion in suspensions of erythrocytes. Therefore, the PFG NMR analysis of water permeability of human erythrocytes

may be useful for the clinical diagnosis of liver disease, and hypo-, or hypercholesterolaemia, all of which affect the C/P ratio of erythrocyte membranes, and presumably that of other cells as well.

Acknowledgements

This work was supported by a grant to P.W.K. and A.R. W. from the Cooperative Research Centre (CRC) for Biomolecular Engineering and Technology; Biosensors and Clinical Diagnostics, and a grant to D.R.S. and M.H.N.-S. from the Royal Prince Alfred Hospital. Dr W.A. Bubb is thanked for help with the NMR spectrometer, and Mr. B.T. Bulliman and Mr. W.G. Lowe are thanked for computing and expert technical assistance, respectively. Ms Alison J. Lennon is thanked for critical reading of the manuscript. Professor Jörg Kärger is kindly thanked for supplying reprints and a copy of the relevant parts of his doctoral thesis.

References

[1] S.-T. Tsai, R. Zhang and A.S. Verkman, Biochemistry, 30 (1991) 2087.
[2] R.A. Garrick, U.S. Ryan, V. Bower, W.O. Cua and F.P. Chinard, Biochim. Biophys. Acta, 1148 (1993) 108.
[3] M. Shporer and M.M. Civan, Biochim. Biophys. Acta, 385 (1975) 81.
[4] G. Benga, O. Popescu, V. Borza, V.I. Pop and A. Hodârnau, J. Membr. Biol., 108 (1989) 105.
[5] M.D. Herbst and J.H. Goldstein, Am. J. Physiol., 256 (1989) C1097.
[6] C. Gasparovic and N.A. Matwiyoff, Magn. Res. Med., 26 (1992) 274.
[7] R.L. Cooper, D.B. Chang, A.C. Young, C.J. Martin and B. Ancker-Johnson, Biophys. J., 14 (1974) 161.
[8] J. Andrasko, Biochim. Biophys. Acta, 428 (1976) 304.
[9] Z.H. Endre and P.W. Kuchel, Biophys. Chem., 24 (1986) 337.
[10] A.S. Verkman, Annu. Rev. Physiol., 54 (1992) 97.
[11] B.L. Smith and P. Agre, J. Biol. Chem., 266 (1991) 6407.
[12] J.M. Verbavatz, D. Brown, I. Sabolic, G. Valenti, A.N. van Hoek, T. Ma and A.S. Verkman J. Cell. Biol., 123 (1993) 605.
[13] A.N. van Hoek, M.L. Hom, L.H. Luthjens, M.D. de Jong, J.A. Dempster and C.H. van Os J. Biol. Chem., 226 (1991) 16633.
[14] M.L. Zeidel, A. Albalak, E. Grossman and A. Carruthers, Biochemistry, 31 (1992) 589.
[15] A. Finkelstein and A. Cass, Nature, 216 (1967) 718.
[16] R.I. Sha'afi, C. Gary-Bobo and A.K. Solomon, Biochim. Biophys. Acta, 173 (1969) 141.
[17] B. de Kruijff, R.A. Demel and L.L.M. van Deenen, Biochim. Biophys. Acta, 255 (1972) 331.
[18] R.A. Demel, K.R. Bruckdorfer and L.L.M. van Deenen, Biochim. Biophys. Acta, 255 (1972) 321.
[19] M. Grunze and B. Deuticke, Biochim. Biophys. Acta, 356 (1974) 125.
[20] B. Deuticke and C. Ruska, Biochim. Biophys. Acta, 433 (1976) 638.
[21] M. Grunze, B. Forst and B. Deuticke, Biochim. Biophys. Acta, 600 (1980) 860.
[22] H. Kutchai, R.A. Cooper and R.E. Forster, Biochim. Biophys. Acta, 600 (1980) 542.
[23] M.J.B. Kutryk and G.N. Pierce, J. Biol. Chem., 263 (1988) 13167.
[24] L.V. Schagila, Y.E. Korchev, A.E. Grinfeldt, A.A. Lev and K. Blaskó, Biochim. Biophys. Acta, 1109 (1993) 91.
[25] M. Bloom, E. Evans and O.G. Mouritsen, Q. Rev. Biophys., 24 (1991) 293.
[26] P.R. Cullis and M.J. Hope, in D.E. Vance and J. Vance (Eds.), Biochemistry of Lipids, Lipoproteins and Membranes, Physical Properties and Functional Roles of Lipids in Membranes, Elsevier, Amsterdam, 1991, p. 1.
[27] H. Brockerhoff, Lipids, 9 (1974) 645.
[28] D.W. Deamer and J. Bramhall, Chem. Phys. Lipids, 40 (1986) 167.
[29] D.W. Deamer and J.W. Nichols, J. Membr. Biol., 107 (1989) 91.
[30] A. Carruthers and D.L. Melchior, Biochemistry, 22 (1983) 5797.
[31] A. Carruthers and D.L. Melchior, Biochemistry, 23 (1984) 6901.
[32] R.A. Cooper, M. Diloy-Puray, P. Lando and M.S. Greenberg, J. Clin. Invest., 51 (1972) 3182.
[33] Y. Levy, R. Leibowitz, M. Aviram, J.G. Brook, U. Cogan, Br. J. Clin. Pharmac., 34 (1992) 427.
[34] J. Kärger, Ann. Phys., 24 (1969) 1.
[35] J. Kärger, Ann. Phys., 27 (1971) 107.
[36] J. Kärger, Adv. Coll. Interf. Sci., 23 (1985) 129.
[37] J. Kärger, H. Pfeiffer and W. Heink, in J.S. Waugh, (Ed.), Advances in Magnetic Resonance, Principles and Application of Self-diffusion Measurements by Nuclear Magnetic Resonance, Vol. 12, Academic Press, San Diego, CA, 1988, p. 51.
[38] C.M. Gary-Bobo and A.K. Solomon, J. Gen. Physiol., 52 (1968) 825.
[39] J. Kärger, PhD Thesis, Karl Marx Universität, Berlin (1970).
[40] J. Kärger, Z. Phys. Chem. (Leipzig) 248 (1971) 27.
[41] J.E.M. Snaar and H. van As, Biophys. J., 63 (1992) 1654.
[42] M.H. Nouri-Sorkhabi, B.E. Chapman, D.R. Sullivan and P.W. Kuchel, Magn. Reson. Med., 32 (1994) 505.
[43] R.A. Cooper, M.H. Leslie, S. Fischkoff, M. Shinitzky, S.J. Shattil, Biochemistry, 17 (1978) 327.

[44] P.W. Kuchel and B.E. Chapman, J. Magn. Reson., 94 (1991) 574.
[45] A.R. Waldeck, A.J. Lennon, B.E. Chapman and P.W. Kuchel, J. Chem. Soc., Faraday Trans., 28 (1993) 2807.
[46] S.J. Gibbs and C.S. Johnson, J. Magn. Reson., 93 (1991) 395.
[47] J. Brahm, J. Gen. Physiol., 82 (1983) 1.
[48] R.A. Cooper, E.C. Arner, J.S. Wiley, S.J. Shattil, J. Clin. Invest., 55 (1975) 115.
[49] J.E. Raftos, B.T. Bulliman and P.W. Kuchel, J. Gen. Physiol., 95 (1990) 1183.
[50] M. Kendall and A. Stuart, The Advanced Theory of Statistics, Griffin, London, 1977.
[51] S. Wolfram, Mathematica, Addison–Wesley, Redwood City, CA, 1991.
[52] R.A. Demel and B. de Kruijff, Biochim. Biophys. Acta, 457 (1976) 109.
[53] M.L. Zeidel, S. Nielsen, B.L. Smith, S.V. Ambudkar, A.B. Maunschbach and P. Agre, Biochemistry, 33 (1994) 1606.
[55] H. Borochov, R.E. Abbot, D. Schachter and M. Shinitzky, Biochemistry, 18 (1979) 251.
[56] R. Mills, J. Phys. Chem., 77 (1973) 685.
[57] P.G. Nilsson and B. Lindman, J. Phys. Chem., 87 (1983) 4761.
[58] B. Jönsson, H. Wennerström, P.G. Nilsson and P. Linse, Coll. Pol. Sci., 264 (1986) 88.